Use of Artificial Potential Fields for UAV Guidance and Optimization of WLAN Communications

Douglas P. Horner, Anthony J. Healey
Center for AUV Research
Naval Postgraduate School, Monterey CA 93943

Abstract: Wireless Local Area Networks (WLAN) are quickly becoming an important part of regional military operations**.** The use of standardized internet protocols enables a wide variety of vehicles, sensors and personnel to interoperate more effectively. For Autonomous Underwater Vehicles (AUV), they permit a potentially great improvement to distribute outputs from data intensive sensors like sonar and video to observers. For a fleet of AUVs tasked with area underwater search and survey, WLANs can facilitate situational awareness, re-tasking and expedience.

Because of the limited range of the 802.11b 2.4GHz channels, one of the keys to realizing WLAN communications between multiple AUVs and Tactical Operations Centers is the positioning of aerial bridges. Unmanned Aerial Vehicles (UAVs) can be used as the platform and moreover sensory based autopilot navigation can be developed to optimize the throughput rate for multi-link data transfers. Artificial Potential Function (APF) methods can be used for guidance law development, once antenna and signal strength models become available. This paper will discuss the results from the recent Naval Postgraduate School (NPS) Surveillance Targeting and Acquisition Network (STAN) experiment conducted at Camp Roberts, CA and follow-on Office of Naval Research (ONR) sponsored Joint Training Fleet Exercise (JTFEX) experiments at Camp Lejuene, NC. Vehicles used in the experiments include the NPS ARIES AUV and Tactically Expendable Remote Navigator (TERN) UAV.

I. Introduction

AUV operations can quickly generate large volumes of oceanographic data. Typically users wait for individual vehicles to complete a mission and return to the host ship before data is accessible. When communication links are available, data can be remotely transferred but the limited bandwidth severely restricts the quantity of data transmitted. While at times, the available bandwidth may be enough to convey the essential information, there are a variety of situations where a higher bandwidth communication channel is required. They include:

1. *Expediency*. Gaining a more thorough understanding of the environment more quickly.
2. *Facilitating Coordinated Behaviors*. Use of the UAV to coordinate the behaviors of a large group of ground and sea-based unmanned systems through re-tasking and monitoring.
3. *Facilitating longer duration missions*. Without having to download the data aboard ship, the AUVs are free to operate for longer periods of time.

For these reasons and others, it makes sense to develop and investigate improved communication links for unmanned systems and to develop the means to autonomously maximize the data throughput and reliability.

II. Artificial Potential Fields for Autonomous Aerial Navigation

Artificial Potential Field (APF) work draws from the potential field theory concept in physics and models obstacles with a repellant force with the navigation goal with an attractive force. Path planning and robot navigation is conducted by minimizing the potential energy in the vector field. The approach was originally developed by Khatib [1] for manipulation of robotic arms and later adapted for mobile robot platforms by J.C. Latombe [2].

Traditionally APFs have been used for obstacle avoidance reactive behaviors but modifications were required to overcome several limitations. These include: Trap situations due to local minima, difficulties in negotiating paths between closely spaced obstacles, navigational oscillations due to the presence of obstacles (especially in narrow passages) [3]. Recent improvements have focused on minimizing the inherent problems with APF methods. One approach introduced a two-layer architecture - a local path planner monitors the robot's path but when a local minima or trap situation occurs a global path planner is invoked for planning a new path.

For the application of maximizing data transfer rates between unmanned systems, APF is potentially a rewarding technique for autopilot control. Simply

Report Documentation Page

Form Approved
OMB No. 0704-0188

1. REPORT DATE **2005**	2. REPORT TYPE	3. DATES COVERED **-**
4. TITLE AND SUBTITLE **Use of Artificial Potential Fields for UAV Guidance and Optimization of WLAN Communications**		5a. CONTRACT NUMBER 5b. GRANT NUMBER 5c. PROGRAM ELEMENT NUMBER
6. AUTHOR(S)		5d. PROJECT NUMBER 5e. TASK NUMBER 5f. WORK UNIT NUMBER
7. PERFORMING ORGANIZATION NAME(S) AND ADDRESS(ES) **Naval Postgraduate School,Center for AUV Research,Monterey,CA,93943-5000**		8. PERFORMING ORGANIZATION REPORT NUMBER
9. SPONSORING/MONITORING AGENCY NAME(S) AND ADDRESS(ES)		10. SPONSOR/MONITOR'S ACRONYM(S) 11. SPONSOR/MONITOR'S REPORT NUMBER(S)

12. DISTRIBUTION/AVAILABILITY STATEMENT
Approved for public release; distribution unlimited

13. SUPPLEMENTARY NOTES
The original document contains color images.

14. ABSTRACT
Wireless Local Area Networks (WLAN) are quickly becoming an important part of regional military operations. The use of standardized internet protocols enables a wide variety of vehicles, sensors and personnel to interoperate more effectively. For Autonomous Underwater Vehicles (AUV), they permit a potentially great improvement to distribute outputs from data intensive sensors like sonar and video to observers. For a fleet of AUVs tasked with area underwater search and survey, WLANs can facilitate situational awareness, retasking and expedience. Because of the limited range of the 802.11b 2.4GHz channels, one of the keys to realizing WLAN communications between multiple AUVs and Tactical Operations Centers is the positioning of aerial bridges. Unmanned Aerial Vehicles (UAVs) can be used as the platform and moreover sensory based autopilot navigation can be developed to optimize the throughput rate for multilink data transfers. Artificial Potential Function (APF) methods can be used for guidance law development, once antenna and signal strength models become available. This paper will discuss the results from the recent Naval Postgraduate School (NPS) Surveillance Targeting and Acquisition Network (STAN) experiment conducted at Camp Roberts, CA and follow-on Office of Naval Research (ONR) sponsored Joint Training Fleet Exercise (JTFEX) experiments at Camp Lejuene, NC. Vehicles used in the experiments include the NPS ARIES AUV and Tactically Expendable Remote Navigator (TERN) UAV.

15. SUBJECT TERMS

16. SECURITY CLASSIFICATION OF:			17. LIMITATION OF ABSTRACT	18. NUMBER OF PAGES	19a. NAME OF RESPONSIBLE PERSON
a. REPORT **unclassified**	b. ABSTRACT **unclassified**	c. THIS PAGE **unclassified**		**8**	

described, the concept is to use the UAV to measure signal strengths from the available, WLAN enabled AUVs and the intersection of the measured signal strengths is used as the attractive force for UAV navigation. This ensures that the resultant UAV position locates and maintains optimal position for data transfer. The process would be described as follows.

An oceanographic operations area is determined for the simultaneous deployment of AUVs. For the purposes of this paper, the vessels at sea (and ashore) are considered the surface nodes in the network. The aerial node is the UAV, which measures the signal strength of the surface nodes either through prior testing or over-flights of the surface nodes. To begin, the UAV is first launched from the ship and transits to the center of the AUV operations area using waypoint navigation. Throughout, this process waypoint navigation remains the default method of navigation.

Once in the operations area, the UAV waits for AUVs to surface and associate into the WLAN. AUVs also signify entry into the network by transmitting their GPS position via Freewave 900 MHz radio. Surface time could also be minimized by pre-scheduling AUV surface times. Once this message is acknowledged, a rough mid-point estimate is calculated between the ship and AUV. A vector field is then constructed based upon the bearing and distance to the point and navigation changes to the APF methodology.

When the UAV is in transit to the approximated mid-point position, it uses a signal strength calculation of the intersection between the distributions to initialize the attractive force for the autopilot navigation. When the UAV approaches the mid-point, the measurements between the actual signal strengths of the mother ship and AUV are used for APF autopilot navigation. Maximal turning radius is preset in the autopilot so that when the UAV is close to the optimal position (where data transfer rate is greatest), a loitering behavior is created by maintaining a safe turning radius.

As additional vehicles surface for transmitting collected data (conversely after they have completed a download and submerge), the procedure continually updates. For vehicles that surface, another GPS location is sent to the UAV. Aboard the UAV, a calculation is made on whether to navigate to a new optimal position. The decision on whether to re-position is predicated on the intersection of the number of nodes in the network. If there is a reasonable solution to the intersecting signal strengths, the vehicle moves into the new position using the methodology described above. If not, the latest node to enter the network is put in a queue or the AUV submerges and continues on its mission. Conversely, if the AUV finishes the data transmission and submerges (and is removed from the queue), the UAV calculates its new position based on the queue and navigates to the new optimal position. If the queue is empty, the UAV defaults to waypoint navigation.

III. Mathematical Analysis for APF Autopilot Navigation

For initial analysis the simplest case is presented where there is one AUV surfaced for a total of 3 network nodes (Support ship, UAV and AUV). Consider the region ? which represents a two-dimensional (x, y) Cartesian plane. When the APF is enacted (when an AUV surfaces / is in the queue) vehicle motion is directed by

$$V(x,y) > 0 \;\; \forall (x,y) \in \Omega \tag{1}$$

where V is single-valued function that has continuous derivatives. Consider a simple motion model for UAV vehicle steering with no side slip where the turn rate k is proportional to the steering command ($a_r(t)$), u is surge or forward speed and ? is heading.

$$\dot{x} = u \cos y \tag{2}$$

$$\dot{y} = u \sin y \tag{3}$$

$$\dot{y} = r = k a_r(t) \tag{4}$$

A guidance law is designed such that $\dot{V}(x,y) > 0$, (in this case we are hill climbing) so that

$$(\frac{\partial V}{\partial x})\dot{x} + (\frac{\partial V}{\partial y})\dot{y} \geq 0; \tag{5}$$

$$\therefore \; \dot{x}(\frac{\partial V}{\partial x}) \geq 0 \;\; and \;\; \dot{y}(\frac{\partial V}{\partial y}) \geq 0 \tag{6}$$

$$a_r(t) = K_p(y_{com} - y) \tag{7}$$

where K_p is heading error gain and $?_{com}$ is the commanded heading. Making each term in equation 5 is greater than or equal to zero ensures that the entire equation is less than zero

$$\dot{x} = l_x(\frac{\partial V}{\partial x}),\; \dot{y} = l_y(\frac{\partial V}{\partial y}) \tag{8}$$

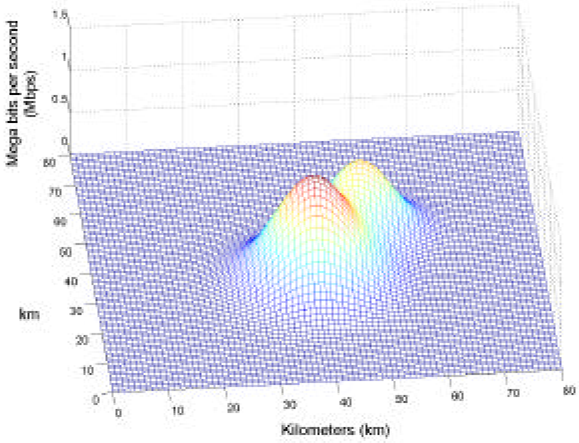

Figure 1. Additive signal strengths

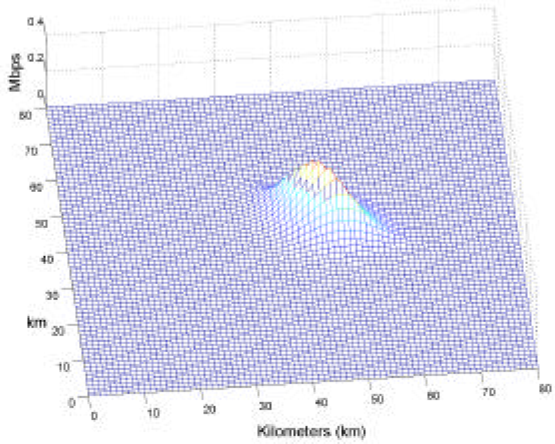

Figure 2. Intersection of two signal strengths

and lambda is the bandwidth or speed of the response measurement. This provides the direction command for the UAV.

$$y = \tan^{-1}(l_y(\frac{\partial V}{\partial y}), l_x(\frac{\partial V}{\partial x})) \qquad (9)$$

The next step is to represent the attractive force which is the intersection of the signal strength characterization of the support ship and the AUV (See Figures 1 and 2). To represent the total vector field and determine the three-dimensional shape of the signal, the following assumptions are made. First, the total vector field is a combination of the upward sloping plane and the joining or intersection of the available signal strengths in the vector field, where V_f is the vector field and V_s is a representation of each signal strength.

$$V_{total} = V_f + \bigcap_i^{\infty} V_s \qquad for\, i = 1..\infty \qquad (10)$$

Second, each of the signal strengths of the two WLAN nodes are two-dimensional Gaussian functions represented by the following equation,

$$V_i = t\,e^{\frac{-(x-x_i)^2}{s_x^{\,2}} + \frac{-(y-y_i)^2}{s_y^{\,2}}} \qquad (11)$$

where x_i, y_i $(for\, i = 1,2)$, are the positions of the unmanned systems, s_x and s_y is the variance in the respective directions and x, y is the position of the UAV and t is a scaling factor representing the maximum data transfer rate.

Third, the resulting intersection of the Gaussian signal strength distributions is also a Gaussian distribution. The resulting volume can be approximated and mapped into the vector field by determining the orientation of the volume and the dimensions along the major and minor axes. This approximated equation is then placed into the artificial vector field through an Euler transformation (z axis rotation) in the xy plane.

Calculation of the orientation of the intersecting volume is accomplished by finding the solution to the following equations:

$$bV_1 - V_2 = 0 \qquad (12)$$

$$t_1 e^{\frac{-(x-x_1)^2}{s_{x_1}^{\,2}} + \frac{-(y-y_1)^2}{s_{y_1}^{\,2}}} = t_2 e^{\frac{-(x-x_2)^2}{s_{x_2}^{\,2}} + \frac{-(y-y_2)^2}{s_{y_2}^{\,2}}} \qquad (13)$$

where the scalar variable ß represents a power ratio between the output of the two transmitters. Setting $t_1 = t_2 = ß = 1$, and taking the natural logarithm of both sides, the general solution to the equation is quadratic.

$$\begin{aligned} & x^2(-s_{x_1}^{-2} + s_{x_2}^{-2}) + 2x(s_{x_1}^{-2}x_1 + s_{x_2}^{-2}x_2) \\ & + y^2(-s_{y_1}^{-2} + s_{y_2}^{-2}) + 2y(s_{y_1}^{-2}y_1 + s_{y_2}^{-2}y_2) \qquad (14) \\ & + (-s_{x_1}^{-2}x_1^2 + s_{x_2}^{-2}x_2^2 - s_{y_1}^{-2}y_1^2 + s_{y_2}^{-2}y_2^2) = 0 \end{aligned}$$

If the variances of the Gaussian functions are equal ($s_{x1} = s_{x2} = s_{y1} = s_{y2}$) the quadratic simplifies to a linear equation.

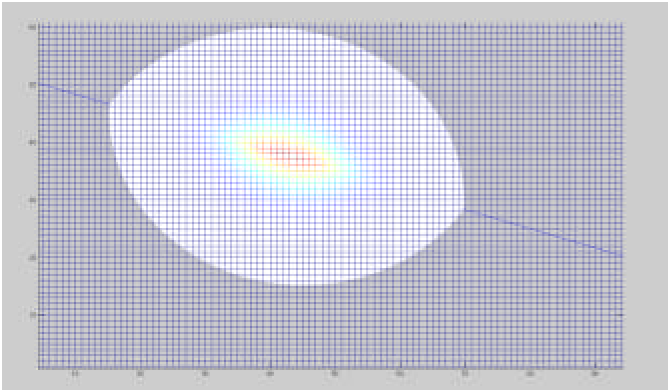

Figure 3. Combined signal strength volume with linear solution

$$y = -\frac{(x_1 - x_2)}{(y_1 - y_2)}x + \frac{(x_1^2 - x_2^2 + y_1^2 - y_2^2)}{2(y_1 - y_2)} \tag{15}$$

$$m = \frac{-(x_1 - x_2)}{(y_1 - y_2)} \tag{16}$$

The extreme points of the solution set (where V_1 and V_2 are both equal to zero) are used for determining the distance along the major axis (used to represent variance in the x direction) and equation 15 is used for determining the angular orientation of the volume for placement into the total vector field. If the solution is quadratic, the angular orientation is formed by a linear approximation of the quadratic function using a least squares fit. Figure 3 shows an example of intersecting Gaussian functions (assuming variances are equal) with a linear solution overlay.

For the minor axis the maximum point of the resulting intersection between the two Gaussian functions is located on the line that is formed between the locations of the two surface nodes. The solution to the point of intersection between the linear equations of the major and minor axis is $\max \bigcap V_s(x,y)$. The length of the minor axis is determined by starting at the maximum point of V_s and progressing along each side of the line until the differential nominally approaches zero.

Alternatively, the length of the minor axis can be approximated by recognizing that if the variances are equal and within reasonable distances between nodes, there is a linear relationship between surface nodes and the length of the minor axis. In other words, as the distance increases between surface nodes the length of the minor axis decreases linearly. In maximum ranges, the length of the minor axis reaches a steady state. The length of the minor axis can then be roughly calculated using equation 17.

$$\begin{aligned} &y = -.4775x + 16.176 \\ &\text{where} \\ &\quad x = \text{ Distance between surface nodes} \\ &\quad \text{y = The length of the minor axis} \end{aligned} \tag{17}$$

With the identification of the length of the major and minor axes and the angular orientation of the combined volume, this can be used to create the Gaussian distribution function to be placed into the total vector field (Figure 4). The function is represented by equation 11 where the lengths of the major and minor axes are used to estimate s_x and s_y and $\max \bigcap V_s(x,y)$ is used as a scaling factor t to represent the maximum data link between the ship and AUV and is the point the UAV flies to while in the APF navigation mode.

The next step is to orient the resulting signal strength function into the total vector field. Two requirements for proper positioning of the Gaussian function are the center point and the angular orientation of the intersecting functions. The center point is $\max \bigcap V_s(x,y)$ and the angular orientation is the slope from equation. This angle is then used for a rotational transformation about the z axis.

$$y = \tan^{-1}(m) \tag{18}$$

$$\begin{pmatrix} x_1 \\ y_1 \\ z_1 \end{pmatrix} = \begin{pmatrix} \cos y & \sin y & 0 \\ -\sin y & \cos y & 0 \\ 0 & 0 & 1 \end{pmatrix} \begin{pmatrix} x_0 \\ y_0 \\ z_0 \end{pmatrix} \tag{19}$$

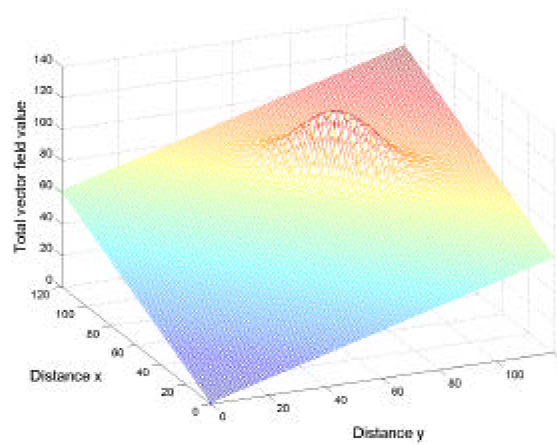

Figure 4. Example of a Total Vector Field

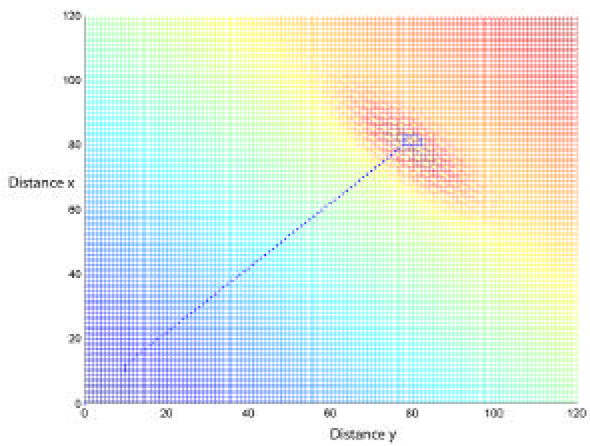

Figure 5. Simulated UAV Navigation using the APF Guidance Methodology

The result of this transformation can then be added to the vector field where the representation of the combined signal strength is centered on the maximal value of the intersection of the two network nodes (ship and AUV) (Figure 4). Figure 5 shows simulated autopilot navigation for an UAV using the described APF methodology in the total vector field.

While the above mathematical analysis for the use of APF for UAV automated navigation is relatively computationally intensive, an algorithm appropriate for real-time UAV control is introduced based on the use of Sliding Mode Control.

IV. Sliding Mode Control

Sliding Mode Control (SMC) is an autopilot technique which navigates to a sliding surface of equilibrium by using different controlling functions in different parts of the system state space. It is appropriate for non-linear systems, is practically easy to use and displays good robustness to uncertainty [4][5][6]. Since it is assumed that the UAV is receiving the signal strength from two surface sources, the line/curve which represents the maximal intersection can be used as the sliding mode point of equilibrium.

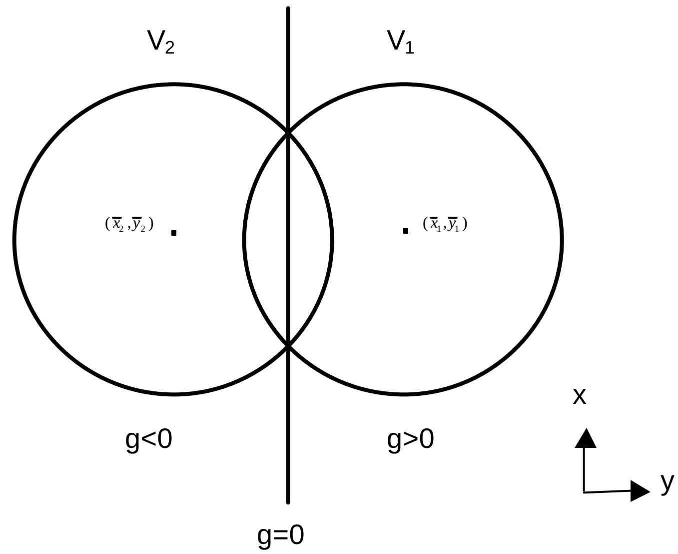

Figure 6

As before, we present the simplified case where there are three nodes in the network, the UAV, the support ship and the surfaced AUV. The AUV and ship have signal strength of the WLAN measured by the UAV and are represented by Figure 6 as V_1 and V_2. These signal strengths are the above described Gaussian functions and if the variances are equal, the linear solution to the intersecting functions is given by equation 19.

$$g = (V_1 - V_2) = 0 \tag{19}$$

At g=0, $V_1 = V_2 = V(x,y)$ and has a single peak. The peak is sought dynamically by a movement given by the velocity vector $[\dot{x}, \dot{y}]^T$ such that V(t) is always increasing. In order to develop a guidance law to enable the UAV to navigate and maintain position over the optimal position data transfer between the AUV and support ship we set up the following optimization problem:

$$\begin{aligned} &\text{Maximize } V_1(x, y) \\ &\qquad \text{subject to:} \\ &\qquad\qquad g = 0 \end{aligned} \tag{20}$$

This ensures that the UAV travels toward the optimal transmission point and that once in the vicinity it maintains a loitering position around this point. To solve the problem we the method of Lagrange multiplier to form the augmented potential function,

$$V = (V_1 + mg) \tag{21}$$

where μ is the Lagrange multiplier, and seek a control law to maximize V which is required to be always positive and seek $(\frac{\partial x}{\partial t},\frac{\partial y}{\partial t})$ such that $\frac{\partial V}{\partial t}>0,\forall t>0$. Through the assignment of an arbitrary function µ such that (µg)>0 we ensure that the augmented potential function V is positive definite. It follows that

$$m=\mathrm{sgn}(g) \tag{21}$$

In similar fashion to the above analysis and using equation 5, a guidance law is designed such that

$$(\frac{\partial V_1}{\partial x}+\mathrm{sgn}(g)\frac{\partial g}{\partial x})\dot{x}+(\frac{\partial V_1}{\partial y}+\mathrm{sgn}(g)\frac{\partial g}{\partial y})\dot{y}>0\ \ \forall\, t>0 \tag{22}$$

$$\therefore \text{ make } \quad \dot{x}=(\frac{\partial V}{\partial x}+\mathrm{sgn}(g)\frac{\partial g}{\partial x})$$
$$\dot{y}=(\frac{\partial V}{\partial y}+\mathrm{sgn}(g)\frac{\partial g}{\partial y}) \tag{23}$$

where

$$u=\left\|\begin{pmatrix}\dot{x}\\ \dot{y}\end{pmatrix}\right\| \text{ is constant}$$

and from equation 18, the vehicle heading command is given by

$$\tan^{-1}((\frac{\partial V_1}{\partial x}+\mathrm{sgn}(g)\frac{\partial g}{\partial x}),(\frac{\partial V_1}{\partial y}+\mathrm{sgn}(g)\frac{\partial g}{\partial y})) \tag{24}$$

In summary, SMC is an autopilot technique appropriate for UAV navigation to the vicinity of the combined maximum data transfer rate point. The sliding manifold objective function is determined by maximizing one of the signal strengths subject to the constraint of the simultaneous solution to the two WLAN surface nodes (g = 0).

V. Initial Experimental Results

Our first step to achieve this sensor-based UAV navigation, has been to quantify the signal strength of the WLAN from various land and sea nodes. To do this we have conducted a number of experiments and demonstrations. The first series of experiments have been associated with the NPS Surveillance Targeting and Acquisition Network (STAN). The tests were conducted at Camp Roberts, Lake San Antonio and Monterey Bay, CA between December 2003 and May 2004.

The tests included the NPS Acoustic Radio Interactive Exploratory Server (ARIES) AUV, the Tactically Expendable Remote Navigator (TERN) UAV, a support boat, a balloon (surrogate for the UAV) and a tracking antenna. IEEE 802.11b compliant wireless bridges were chosen for the communication link. The commercial technology was low-cost, reliable, readily available and relatively easy to administer. Having the bridges in compliance with the IEEE standard facilitated TCP/IP communications between networked nodes. A maximum theoretical limit on the throughput is 11 Mbps while the actual throughput is typically 3 to 6 mbps.

Table 1 lists some of the equipment in the experiment and Figure 7 summarizes the network topology. Of note, the TERN, balloon and tracking antenna all used 900 MHz Freewave radios. They were used to transmit the GPS position of either the TERN or balloon to the tracking antenna. This permitted the tracking antenna to maintain a solid fix on the position of the aerial node. The tracking antenna provided the longest link and at maximal ranges accounted for up to 80% of the total distance. Throughout the following tests the link was tested using (Moving Picture Experts Group) MPEG video files of various sizes (2-24MB).

Vehicle	Antenna type	Antenna gain (dBi)	Duration (hours)
ARIES	Omni-directional	3	4
TERN	Omni-directional	2	4
Whaler	Omni-directional	2	48
Balloon	Omni-directional	3	48
Operations Center	Tracking/ Directional	14	Unlimited

Table 1 List of Communications Characteristics

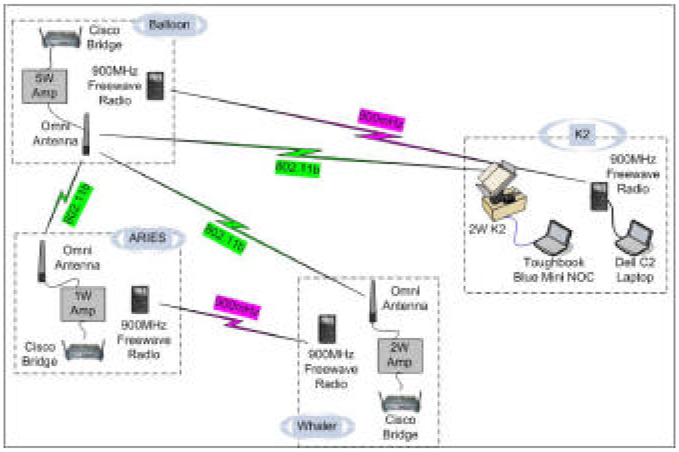

Figure 7 Network Links

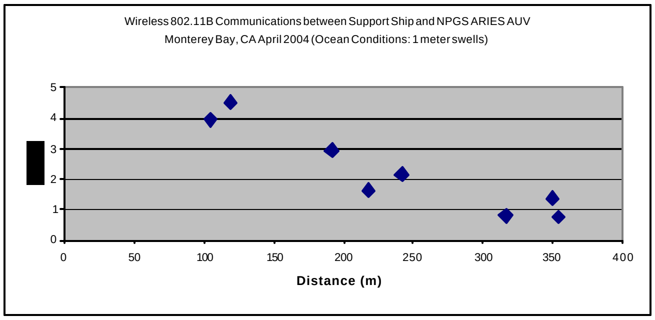

Figure 8

Figure 8 shows a chart of the data transfer rate between a support vessel and the ARIES. The support vessel configuration was identical to the support vessel with the exception that the antenna was located at approximately 8 meters above sea level. With just one link between the two nodes the data rates were considerable higher than when multiple links are required.

The STAN testing culminated in the May 2004 experiment where a test of the full UUV-UAV-Operations Center link was accomplished. With the ARIES vehicle in Lake San Antonio and the TERN flying 4km from ARIES a test was conducted from the which permitted wireless communications data transfer from the ARIES through the UAV to the command center for a total distance of 13km. The average speed for the file transfers was 243 kbps.

The most recent set of experiments occurred in June 2004 with the Office of Naval Research Organic Mine Countermeasure (OMCM) technology demonstration at the US Marine Corp Base Camp LeJeune, NC . Over the course of ten days, demonstrations and experiments were conducted to determine the maximum link distances and the data transmittal rates at various distances.

The maximum distance achieved from the tracking antenna to the support vessel was 28km. Of that distance 20km was from the tracking antenna to the balloon and 8km was from the balloon to the whaler boat. Figures 9 and 10 shows the link between the balloon (at 330 meters elevation) and boat as the boat navigated to sea away from the balloon. Total data transfer rates (150-400 kbps) were less than had been seen in previous experiments and this is attributed to the extreme distance between the tracking antenna and balloon.

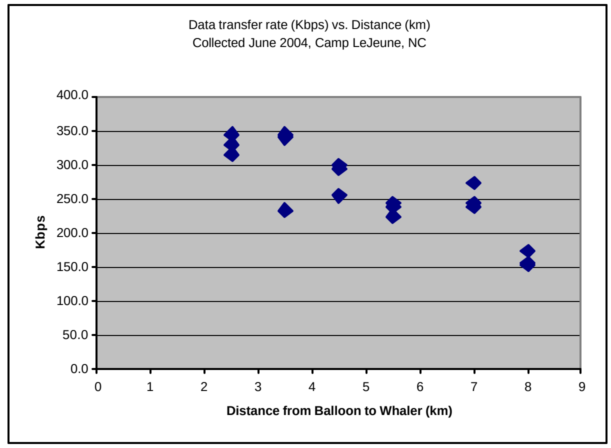

Figure 9

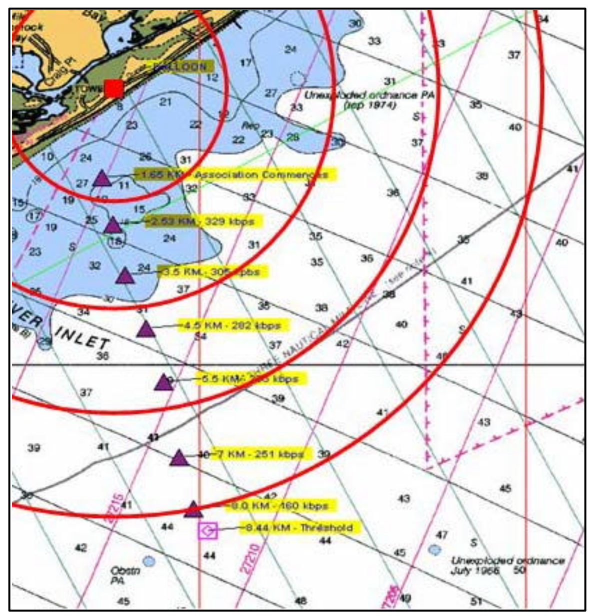

Figure 10.

VI. Conclusions

In this paper, we introduced the idea of using WLANs to facilitate the passing of collected oceanographic data from a team of AUVs. In certain applications, higher bandwidth communications can significantly improve collaborative AUV operations. With the limited distances available with higher frequencies it makes sense to use aerial vehicle as a communication bridge to extend transmission ranges. If there is a device measuring multiple signal strengths aboard the UAV, one can use this information to navigate and maintain position over the point which has the maximum data transfer rate. A methodology using APF and SMC was shown as a potential robust solution for sensory based autopilot navigation. Finally empirical results were reported on initial field tests with surface and aerial nodes.

VII. Acknowledgments

The Center of AUV Research would like to acknowledge the sponsorship of Dr. Tom Swean with the Office of Naval Research under contract number N0001404WR.

VIII. References

[1] O. Khatib, "Real-time obstacle avoidance for manipulators and mobile robots," Int. J. Robot. Res.,vol. 5, no. 1, pp. 90-98, 1986

[2] J.C. Latombe *Robot Motion Planning*, Kluwer Academic Publishers, Boston, 1991.

[3] Korem, Y. and Borenstein J. "Potential Field Methods and Their Inherent Limitations." Proceedings of the 1991 IEEE International Conference on Robotics and Automation, Sacramento, CA – April 1991 pp. 1398-1403.

[4] R. Cristi, F.A. Papoulias, and A.J. Healey, "Adaptive sliding mode control of autonomous underwater vehicles in the dive plane," IEEE J. Oceanic Eng. Vol. 15, pp. 462-470, 1991.

[5] A.J. Healey, D. Lienard, "Multivariable Sliding Mode Control for Autonomous Diving and Steering of Unmanned Underwater Vehicles", IEEE J. Oceanic Eng. Vol. 18, pp. 327-339, 1993.

[6] R.A. DeCarlo, S.H. Zak and G.P. Matthews, "Variable Structure Control of Nonlinear Multivariable Systems: A Tutorial", Proceedings of the IEEE, Vol. 76 No. 3, March 1988, p. 212-232.

Douglas Horner received his Baccalaureate at Boston University with a dual degree in Math and Economics. He spent 12 years as an active duty Naval Special Warfare Officer gaining practical experience in diving and underwater robotics. In 1997 he received his M.S. degree in Applied Mathematics and M.A. degree in National Security Affairs at the Naval Postgraduate School. Since 2001, he has worked as a Research Associate at the Naval Postgraduate School principally with the Center for Autonomous Underwater Vehicles. His main research areas are Artificial Intelligence applications to robotic systems and Machine learning.

Dr. Anthony Healey To be provided